Collapse of a Charge-Ordered State under a Magnetic Field in $Pr_{1/2}Sr_{1/2}MnO_3$

Y. Tomioka,[1] A. Asamitsu,[1] Y. Moritomo,[1] H. Kuwahara,[1] and Y. Tokura[1,2]

[1]*Joint Research Center for Atom Technology, (JRCAT), 1-1-4 Higashi, Tsukuba 305, Japan*
[2]*Department of Physics, University of Tokyo, Hongo Bunkyo-ku, Tokyo 113, Japan*

(Received 13 February 1995)

The perovskite-type manganese oxide, $Pr_{1-x}Sr_xMnO_3$ ($x = 0.5$), shows a first-order phase transition from a ferromagnetic (FM) metal to antiferromagnetic (AFM) nonmetal at 140 K, which accompanies the transition to the charge-ordered state (generalized Wigner lattice). The nonmetal-to-metal transition temperature can be decreased down to near 0 K with a magnetic field up to 70 kOe. The temperature-field phase diagram for the charge-ordered state is presented together with a discussion on the mechanism of this field-induced phase transition.

PACS numbers: 71.27.+a, 71.28.+d, 71.30.+h, 75.30.Kz

The phenomenon of real-space ordering of charge carriers in crystals takes place when the long-range Coulomb interaction among the carriers overcomes the kinetic energy of the carriers. Such a charge-ordering state is occasionally observed in reduced dimensions or when the carrier concentration is a certain fraction ($\frac{1}{8}, \frac{1}{3}, \frac{1}{2}$, etc.) of the number of lattice points in the narrow-band system. Many such examples are seen in $3d$ transition metal oxides: For example, the Verwey transition [1] in Fe_3O_4 corresponds to the real-space ordering of Fe^{2+} and Fe^{3+} species. Such ordering of polarons has also been reported for hole-doped transition metal oxides with a layered perovskite structure, such as $La_{2-x}Sr_xNiO_4$ ($x = \frac{1}{3}$ and $\frac{1}{2}$) [2] and $La_{1-x}Sr_{1+x}MnO_4$ ($x = \frac{1}{2}$) [3]. In this Letter, we describe the discovery of new phenomena relevant to the charge-ordering phase transition in the hole-doped manganese oxide, that is, the collapse of the charge-ordering state under an external magnetic field, which accompanies drastic changes in the electronic and magnetic properties. The charge-ordered lattice (generalized Wigner lattice) can be melted even at zero temperature by a magnetic field.

Among a number of transition metal oxides, $La_{1-x}Sr_xMnO_3$ and $La_{1-x}Ca_xMnO_3$ have long been known as ferromagnetic (FM) conductors [4–6]. Hole doping in the antiferromagnetic (AFM) insulator $LaMnO_3$ (Mn^{3+}; $t_{2g}^3e_g^1$) by substitution of La sites with alkaline earth elements induces an insulator-to-metal (IM) transition. Doped charge carriers (e_g holes) mediate the FM interaction between localized t_{2g} spins, which is known as the double exchange interaction [7,8]. Recent investigations [9–13] have revealed that these hole-doped manganese oxides show giant negative magnetoresistance (MR) phenomena and strong spin-charge coupling.

In general, a perovskite shows an orthorhombic distortion, accompanying the alternative buckling of, say MnO_6, octahedra, when the perovskite A site ionic radius becomes smaller (e.g., La → Pr) or the tolerance factor smaller. [The tolerance factor is defined as $(r_B + r_O)/\sqrt{2}(r_A + r_O)$, where r_A, r_B, and r_O are the ionic radii of the A site, B site, and oxygen ions, respectively.] Such a Mn-O-Mn bond angle distortion effectively reduces the transfer interaction of e_g electrons (holes), as is well known for other perovskites of $3d$ transition metal oxides [14]. Previous investigations [15–17] on some of the perovskite-type Mn-oxide families with smaller transfer interaction of e_g electrons, e.g., $Pr_{1-x}Ca_xMnO_3$ and $Pr_{1-x}Sr_xMnO_3$, have revealed that the charge-ordering effect, i.e., the regular arrangement of $Mn^{3+} : Mn^{4+}$ in 1:1 ratio, plays another important role in the electronic and magnetic properties. The compound $Pr_{1-x}Sr_xMnO_3$ investigated here has been known as a conducting ferromagnet for $0.3 \leq x \leq 0.4$ [17]. For the $x \approx 0.5$ (ceramics) sample, however, neutron diffraction studies [17] have shown that the charge-ordered state prevails at low temperatures. At the transition from the FM to the AFM charge-ordered state, an abrupt change in lattice parameters of the orthorhombic crystal has also been observed [17].

Thus the electronic properties of the perovskite-type $R_{1-x}A_xMnO_3$ critically depend on both the bandwidth and the filling $(1 - x)$. Unique for the hole-doped manganese oxides is that the charge dynamics is highly correlated with the spin dynamics in terms of the double exchange interaction and hence controllable to some extent by an external magnetic field. It was found in this study that with application of the external magnetic field the charge-ordered state in a $Pr_{1/2}Sr_{1/2}MnO_3$ crystal undergoes a sort of "melting" transition of the first order, accompanying hysteretic jumps in resistivity.

Crystals of $Pr_{1-x}Sr_xMnO_3$ ($x = 0.5$) were melt-grown in air with the use of the floating-zone furnace, which is equipped with two halogen incandescent lamps and double hemiellipsoidal mirrors. The growth rate was 5–7 mm/h with the feed and seed rods rotated in opposite directions at 30–40 rpm. X-ray powder diffraction analysis indicated no impurity phase in the crystals grown, and ICP (inductively coupled plasma) mass spectrometry revealed that the cation ratio of Sr to Pr in the crystal was 54/55. The spatial homogeneity of Sr content (x) in the crystal was further checked by the electron-probe-microanalysis technique, which indicated x within ± 0.01. The middle part of the single crystal was cut out

0031-9007/95/74(25)/5108(4)$06.00

and used for the measurements. To release thermal strain, the as-grown crystal was annealed at 1200 °C for 35 h in O_2 gas flow and was slowly cooled to room temperature (20 °C/h).

Figure 1 shows the temperature dependence of the resistivity (ρ) in the absence of a magnetic field (upper panel) and the magnetization in ZFC and FC runs taken under 5 kOe (lower panel). The ZFC and FC curves in the lower panel of Fig. 1 indicate the transition to the FM state at $T \approx 270$ K, which is in accord with the anomaly in the ρ-T curve at $T \approx 270$ K shown in the upper panel. With further decrease of temperature, however, the FM magnetization abruptly disappears at $T \approx 140$ K, and, correspondingly, the resistivity shows a jump from a low to a high value. Below $T \approx 140$ K the ρ-T curve becomes semiconducting. In previous work on ceramics samples [17] the metallic regime was not observed for $x = 0.5$, while in our single crystal sample it exists for $T > 140$ K. The difference may originate from the effects of grain boundaries, which are avoided in the present work using a high quality single crystal. Figure 1 indicates that the FM metal state becomes unstable below $T \approx 140$ K and that it is replaced by the charge-ordered state, i.e., the regular arrangement of $Mn^{3+} : Mn^{4+}$ at 1:1, as shown in the inset of Fig. 1 [17]. Such a charge-ordered state is accompanied by AFM ordering (the so-called CE type [18]). The difference in the critical temperatures T_c and T_v in the previous ($T_c \approx 200$ K, $T_v \approx 160$ K) and present ($T_c \approx 270$ K, $T_v \approx 140$ K) studies may be due to a slight difference of the composition of the samples [19].

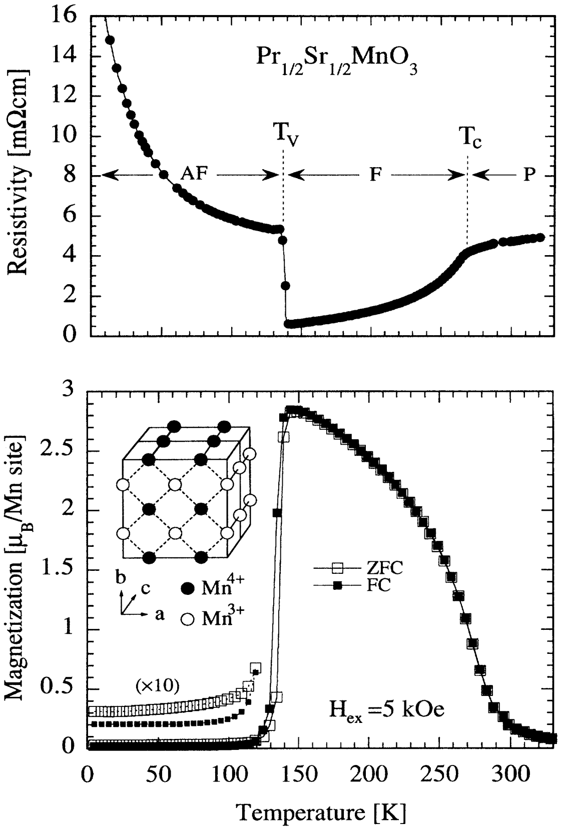

FIG. 1. Upper panel shows the temperature dependence of resistivity (along the c axis) in the absence of magnetic field for a $Pr_{1/2}Sr_{1/2}MnO_3$ crystal. P for $T > T_c$, F for $T_v < T < T_c$ and AF for $T < T_v$ denote paramagnetic, ferromagnetic, and antiferromagnetic states, respectively. Lower panel shows ZFC (zero-field cooled; open squares) and FC (field-cooled; closed ones) magnetization curves under 5 kOe. Both the ZFC and FC curves are magnified for $T < 120$ K. Inset shows the feature of the charge ordering in which only Mn sites are shown (from neutron diffraction on polycrystals [17]).

Figure 2 shows the ρ-T curves taken in the presence of a magnetic field. The resistivity was first measured by cooling the sample from 330 to 4.2 K under a magnetic field (field cooling) and subsequently measured by warming from 4.2 to 330 K at the same constant field [field-cooled warming (FCW)]. In addition to the fairly large negative MR effect around the FM transition temperature (≈270 K), which is similar to the case of $La_{1-x}Sr_xMnO_3$ [7], Fig. 2 shows that the transition point from the FM metal to the AFM charge-ordered state is altered by the applied magnetic field. The transition temperature T_v, tentatively defined as the midpoint of the resistive transition, decreases with an increase in the external magnetic field H. In the case of $H < 50$ kOe, the ρ-T curves below T_v are semiconducting and have nearly

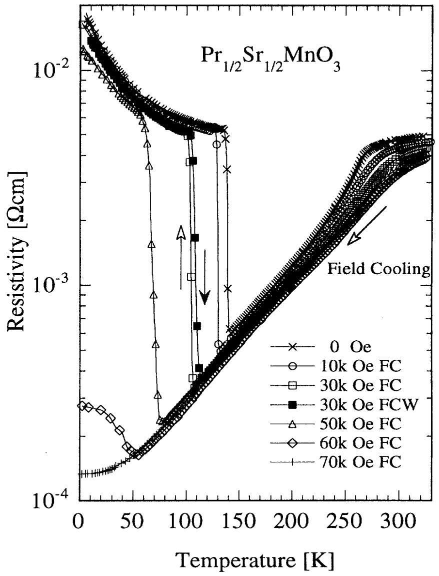

FIG. 2. Temperature dependence of resistivity for $Pr_{1/2}Sr_{1/2}MnO_3$ taken at several magnetic fields. The resistivity was measured by cooling the sample from 330 K to 4.2 K under a magnetic field. For the data at 30 kOe, both FC (field cooling) and FCW (field-cooled warming) runs are shown.

the same value of $\rho \approx 2 \times 10^{-2}\ \Omega\,\mathrm{cm}$ at the lowest temperature. In the case of $H = 70$ kOe, the charge-ordered state completely disappears. Hysteresis between the FC and FCW runs is observed as exemplified by the ρ-T curves under $H = 30$ kOe in Fig. 2 and ensures that the observed sharp transition at T_v is of the first order.

To correlate the charge dynamics with the magnetic structure, the resistivity as well as the magnetization as a function of magnetic field was measured at several fixed temperatures. Figure 3 shows the M-H (upper panel) and ρ-H (lower panel) curves taken at 100 and 120 K. In the M-H curve at 100 K, for example, the magnetization for $0 < H < 28$ kOe in the field-increasing process is characteristic of the AFM state, while that for $H > 38$ kOe changes to that of the FM state with the saturated magnetization of about $3.3\mu_B$ per Mn site [20]. In the subsequent field-decreasing process, the transition from the FM to the AFM state occurs at a slightly lower magnetic field, showing hysteresis between both processes. This metamagneticlike behavior in the M-H curve is in accord with the corresponding ρ-H curve shown in the lower panel of Fig. 3. The resistivity at 100 K in the field-increasing run shows a steep decrease (increase) at ~38 kOe (34 kOe), at which the corresponding magnetization curve changes to (departs from) the FM curve. A similar behavior is also observed for the M-H and ρ-H curves taken at 120 K.

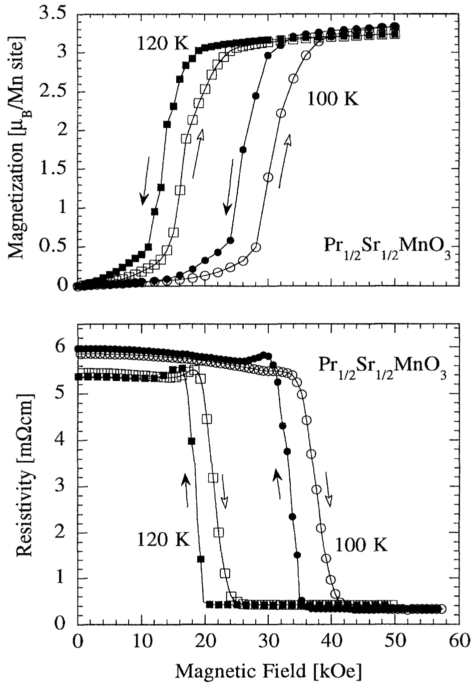

FIG. 3. Magnetization (upper panel) and resistivity (lower panel) for $\mathrm{Pr}_{1/2}\mathrm{Sr}_{1/2}\mathrm{MnO}_3$ taken at 100 and 120 K as a function of magnetic field. Both measurements were performed after the sample was cooled under zero field.

Figure 4 shows the thus determined phase diagram of $\mathrm{Pr}_{1/2}\mathrm{Sr}_{1/2}\mathrm{MnO}_3$. The charge-ordered phase with high resistivity is present in the low-temperature and low-field region. The phase transition is of the first order, accompanied by a hysteresis. The hysteretic region of the magnetic field at a fixed temperature appears to increase at low temperatures, in particular below 60 K, and is as large as 10.1 kOe in width at 4.2 K. The temperature-dependent hysteretic behavior is naturally understood by considering that the thermal fluctuations are suppressed at low temperatures. The phase transition and its magnetic field dependence result, as argued below, from the competition and subtle balance between the kinetic energy gain of the charge carriers in terms of the double exchange interaction and the Coulomb and magnetic energy gain due to the formation of AFM charge-ordered lattice.

In the absence of a magnetic field, the charge-ordering phenomena seem to be the generic properties of $R_{1-x}A_x\mathrm{MnO}_3$ ($x \approx 0.5$) with a relatively narrow e_g electron bandwidth. The feature seems to strongly depend on the ionic radius of (R,A) ions or equivalently on the one-electron bandwidth of the e_g band. In the case of $\mathrm{La}_{1-x}\mathrm{Sr}_x\mathrm{MnO}_3$, the bandwidth of which is considered to be rather wide (and the tolerance factor is 0.94 for $x = 0.5$ [4]), the doping-induced IM transition takes place at $x = 0.17$, but no charge-ordering phase shows up even when the nominal hole concentration is increased up to $x = 0.5$. By contrast, in the case of $\mathrm{Pr}_{1-x}\mathrm{Ca}_x\mathrm{MnO}_3$ with a smaller tolerance factor (0.89 for $x = 0.5$ [4]),

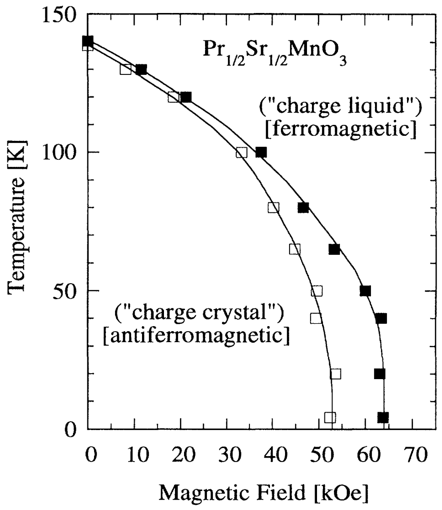

FIG. 4. Magnetic field dependence of the charge-ordering temperature T_v observed for a $\mathrm{Pr}_{1/2}\mathrm{Sr}_{1/2}\mathrm{MnO}_3$ crystal. The transition points are determined by the ρ-H measurements, which is similar to the lower panel of Fig. 3. Closed squares denote the transition from the charge-ordered to the metal state and open ones that from the metal to the charge-ordered state, respectively.

the semiconducting behavior is observed for the whole compositional region of $0 < x < 1$, and the charge-ordering phase is present for a broader range of doping $0.3 < x < 0.7$ around $x = 0.5$. These facts indicate that the charge-ordering instability prevails with a decrease in the transfer (hopping) interaction of e_g holes (electrons); namely, it becomes energetically favorable for doped holes (electrons) to be localized and crystallized due to the repulsive Coulomb interaction among them. The electron-lattice interaction may give rise to an additional energy gain for the charge-ordered lattice (i.e., a polaron lattice).

In the present $Pr_{1-x}Sr_xMnO_3$ with a tolerance factor of 0.93 for $x = 0.5$ [4], in which the electronic situation appears to be between the above two typical materials, the doping-induced IM transition takes place at $x \approx 0.3$ and the charge ordering takes place in the vicinity of $x = 0.5$. In terms of phenomenology, application of a magnetic field (H) apparently tends to stabilize the FM state due to the gain ($-MH$) in the free energy rather than the AFM charge-ordered state ($M \approx 0$). What is specific for $Pr_{1-x}Sr_xMnO_3$ ($x \approx 0.5$) is that the FM metallic and AFM charge-ordered states are nearly degenerate though separated by a potential barrier in the free energy. In fact, such a field-induced phase transition hardly occurs (at least up to 70 kOe) for $Pr_{1-x}Ca_xMnO_3$ ($x \approx 0.5$) in which the AFM charge-ordered state ($M \approx 0$) is perhaps much more stable than the FM state at low temperatures.

Here it is to be noticed that the magnetic-field-induced resistive transition observed in the present study is quite different in nature from the conventional nonmetal-to-metal transition reported for magnetic semiconductors, e.g., EuSe [21,22]. In the magnetic semiconductors, low-density carriers ($n \sim 10^{19}$ cm^{-3}) in the conduction band, which are localized due to coupling with the f-electron spins, traverse the mobility edge upon the application of an external magnetic field, causing a large negative MR at low temperatures. By contrast, the present manganese oxide system has a much higher carrier concentration ($\geq 5 \times 10^{21}$ cm^{-3} as expected for the chemical composition and also confirmed by Hall measurements at low temperatures [23]), which undergoes a sort of crystallization, i.e., charge-ordering transition. Thus the presently observed resistive transition is a consequence of the field-induced phase transition [24] between the "crystal-like" and "liquidlike" states of the doped charges and should be distinguished from the localization-delocalization transition of the one-particle state as in the case of the magnetic semiconductors.

In conclusion, we have found a magnetic field-induced phase transition from the AFM charge-ordered state to the FM metal in a $Pr_{1/2}Sr_{1/2}MnO_3$ single crystal. The phase transition accompanies a large jump in resistivity, which is also viewed as a colossal negative MR. The phase diagram for the charge-ordered state is presented in the plane of temperature and magnetic fields.

The authors are grateful to H. Kawano and H. Yoshizawa for their neutron diffraction measurements and helpful discussions. The authors would like to thank K. Kishio, K. Kitazawa, N. Nonose, Y. Yokoyama, A. Yamada, and H. Akinaga for their help in experiments. This research was supported by NEDO (New Energy and Industrial Technology Development Organization) of Japan.

[1] E. J. W. Verwey, P. W. Haayman, and F. C. Romeijn, J. Chem. Phys. **15**, 181 (1947).
[2] C. H. Chen, S.-W. Cheong, and A. S. Cooper, Phys. Rev. Lett. **71**, 2461 (1993); S.-W. Cheong *et al.*, Phys. Rev. B **49**, 7088 (1994).
[3] Y. Moritomo *et al.*, Phys. Rev. B **51**, 3297 (1995).
[4] G. H. Jonker and J. H. van Santen, Physica **16**, 337 (1950).
[5] G. H. Jonker, Physica **22**, 707 (1956).
[6] C. Zener, Phys. Rev. **82**, 403 (1951).
[7] P. W. Anderson and H. Hasegawa, Phys. Rev. **100**, 675 (1955).
[8] P.-G. de Gennes, Phys. Rev. **118**, 141 (1960).
[9] Y. Tokura *et al.*, J. Phys. Soc. Jpn. **63**, 3931 (1994).
[10] R. M. Kusters *et al.*, Physica (Amsterdam) **155B**, 362 (1989).
[11] K. Chahara *et al.*, Appl. Phys. Lett. **63**, 1990 (1993).
[12] R. von Helmont *et al.*, Phys. Rev. Lett. **71**, 2331 (1993).
[13] S. Jin *et al.*, Science **264**, 413 (1994); M. McCormack *et al.*, Appl. Phys. Lett. **64**, 3045 (1994).
[14] J. B. Torrance *et al.*, Phys. Rev. B **45**, 8209 (1992).
[15] E. Pollert, S. Krupicka, and E. Kuzmicova, J. Phys. Chem. Solids **43**, 1137 (1982).
[16] Z. Jirak *et al.*, J. Magn. Magn. Mater. **15–18**, 519 (1980); Z. Jirak *et al.*, *ibid.* **53**, 153 (1985).
[17] K. Knizek *et al.*, J. Solid State Chem. **100**, 292 (1992).
[18] E. O. Wollan and W. C. Koehler, Phys. Rev. **100**, 545 (1955).
[19] The temperatures T_c and T_v in the vicinity of $x = 0.5$ are quite sensitive to the Sr content. The T_c and T_v for a $x = 0.55$ sample were ≈ 210 and ≈ 205 K, respectively.
[20] The value may include the contribution from Pr^{3+} moments. At such high temperatures (100 and 120 K), however, the Pr^{3+} spins are likely not to be ordered, and the observed magnetization is perhaps predominantly from the Mn spins.
[21] Y. Shapira *et al.*, Phys. Rev. B **10**, 4765 (1974).
[22] T. Kasuya and A. Yanase, Rev. Mod. Phys. **40**, 684 (1968).
[23] A. Asamitsu, Y. Moritomo, and Y. Tokura (unpublished).
[24] K. Bärner, L. Haupt, and R. V. Helmolt, Phys. Status Solidi (a) **187**, K61 (1995).